

Gravitational waves and dark matter with witten effect

Ruiyu Zhou^{a,b} Ligong Bian^{b1}

^a *School of Science, Chongqing University of Posts and Telecommunications, Chongqing 400065, P. R. China*

^b *Department of Physics and Chongqing Key Laboratory for Strongly Coupled Physics, Chongqing University, Chongqing 401331, P. R. China*

E-mail: zhoury@cqupt.edu.cn, lgbycl@cqu.edu.cn

ABSTRACT: We investigate the breaking of dark $SU(2)_d$ symmetry at different temperature scales, occurring after Peccei-Quinn symmetry breaking or following QCD symmetry breaking. We focus on assessing the potential of the hidden monopoles generated during this process to serve as dark matter candidate. Additionally, we examine the impact of axion-monopole interactions on the axion mass. When the phase transition occurs at extremely high temperature ($\sim 10^8 \text{GeV}$), the contribution of monopoles to the axion mass through witten effect becomes non-negligible, playing a crucial role in accurately determining the axion relic density. Moreover, the stochastic gravitational wave background generated by dark phase transition and axionic domain wall collapse may offer a potential explanation for the low-frequency gravitational wave signals observed in PTA experiments.

¹Corresponding Author.

Contents

1	Introduction	1
2	The dark $SU(2)_d$ phase transition	3
3	The Witten effect and the DM relic density	5
4	The gravitational wave and the dark radiation	9
4.1	Gravitational waves from the dark phase transition	10
4.2	Gravitational waves from the domain wall	11
4.3	Dark radiation	13
5	Conclusion and Discussions	13
A	Thermal correction	14

1 Introduction

The successful discovery of gravitational waves has inaugurated a new era in gravitational wave astronomy and provided a novel approach to explore new physics beyond the Standard Model (SM) [22]. Many significant phenomena in the early universe, such as the electroweak phase transition and sphaleron, remain challenging to probe directly due to their occurrence at extremely high energy scales. However, detecting the gravitational wave signals associated with these events offers a promising avenue to deepen people’s understanding of these phenomena. Moreover, considerable research efforts [32, 36–38] have focused on utilizing gravitational wave observatories, such as LIGO [35] and ET [33], to probe gravitational wave signals originating from the Peccei-Quinn(PQ) phase transition, offering a novel pathway for axion detection. Recently, pulsar timing arrays (PTAs) [42, 43, 56, 57] reported a potential detection of a low-frequency stochastic gravitational wave background, sparking considerable interest in exploring its origin, with nanohertz phase-transition gravitational waves [23, 46–55] becoming a focal point of study.

The axion [147, 148] was proposed as one of the most promising solutions to the long-standing strong CP problem in particle physics. As a pseudo-Nambu-Goldstone boson in the PQ symmetry breaking, the axion dynamically cancels the CP phase, providing an elegant solution to the strong CP problem. Moreover, the mass imparted to the axion by the QCD instanton effects [140, 145, 146] makes it one of the compelling candidates for cold dark matter (DM) through the misalignment mechanism[144]. Within this framework, the cosmological abundance of the axion is governed by its mass (or its decay constant f_a , which is closely related to the axion mass and PQ symmetry breaking scale) and the initial misalignment of the axion field, typically expressed as θ_{mis} . Non-perturbative QCD effects

are not the only source of axion mass. Refs. [1, 97–99] have demonstrated that the Witten effect can contribute mass to the axion and significantly influence its dynamics.

The detection of magnetic monopoles has long been a central focus in physics and astronomy. Recently, refs. [11, 13, 44, 45] (see ref. [12] for a recent review) have proposed novel detection methods or experimental constraints for magnetic monopoles. In addition, the potential role of monopoles as topological DM has been extensively explored in refs. [2, 19–21, 27–31, 39, 40, 61, 64]. Furthermore, refs. [24–26] suggest that if the 't Hooft-Polyakov monopole [65, 66] originates from the dark sector, which could significantly contribute to the observed relic density. Additionally, the decay of topological defects, such as magnetic monopoles and domain walls, can generate axions, affecting their cosmological abundance. Moreover, ref. [30] demonstrates that when considering the coupling between monopoles and QCD axions, the Witten effect on the axion abundance becomes non-negligible, particularly before the QCD phase transition. And, ref. [98] illustrates the key role of the interaction between axions and monopoles in alleviating the three-way tension in the pre-inflationary QCD axion DM scenario. This paper investigates the scenario in which the PQ symmetry is broken after cosmic inflation, known as the post-inflationary axion scenario. Under these conditions, spontaneous breaking of the discrete subgroup $Z(N)$ of the $U(1)_{PQ}$ symmetry leads to the formation of topological defects known as domain walls [141]. However, the presence of these domain walls can significantly affect the evolution of the universe, a phenomenon referred to as the domain wall problem [142, 143]. To address this problem, it is generally necessary for the domain walls to collapse before they overclose the universe [83–85]. This collapse process also involves gravitational wave radiation, and detecting these stochastic gravitational wave background signals can provide significant constraints on axion models.

Given the rich phenomenology associated with the $SU(2)_d$ dark sector, a substantial body of literature has already explored cosmological phase transition [23, 41, 59, 110], DM [23, 58, 60, 62, 63, 80–82, 108, 110], and hidden monopole [24, 26, 40]. In this paper, we focus on the hidden monopoles generated by the collisions of vacuum bubbles during a first-order phase transition and the impact of the interaction between hidden monopoles and axions on the axion mass and relic density. We also estimate the stochastic gravitational wave background produced by dark phase transition and domain wall collapse.

This paper is organized as follows. In Sec. 2, we overview the dark $SU(2)_d$ model and the finite temperature effective potential. The Witten effect and the relic density of both monopole and axion will be explored in Sec. 3. Sec. 4 discusses the gravitational wave from the dark phase transition and the domain wall collapse. Our summary is drawn in Sec. 5.

2 The dark $SU(2)_d$ phase transition

The Lagrangian of the dark gauge $SU(2)_d$ symmetry triplet scalar with the PQ symmetry complex scalar:

$$\begin{aligned} \mathcal{L} = & \frac{1}{2}\partial_\mu\varphi^*\partial^\mu\varphi - \frac{1}{4}\lambda(|\varphi|^2 - v_\varphi^2)^2 - \frac{\lambda}{6}T^2|\varphi|^2 \\ & - \frac{1}{4}F_{\mu\nu}^a F^{\mu\nu a} + \frac{1}{2}D_\mu\phi_a D^\mu\phi_a - \frac{\lambda_\phi}{4}(\phi_a\phi_a)^2 - \lambda_{\varphi\phi}|\varphi|^2\phi_a\phi_a, \end{aligned} \quad (2.1)$$

where φ is a complex singlet scalar of the global $U(1)_{PQ}$ symmetry, ϕ_a is a dark $SU(2)_d$ triplet scalar, λ is the PQ coupling constant, and $\lambda_{\varphi\phi}$ is the coupling between the φ and ϕ . Therein, the field strength of the $SU(2)_d$ field A_μ is $F_{\mu\nu}^a = \partial_\mu A_\nu^a - \partial_\nu A_\mu^a + g_d\epsilon^{abc}A_\mu^b A_\nu^c$, the kinetic term is $D_\mu\phi_a = \partial_\mu\phi_a + g_d\epsilon^{abc}A_\mu^b\phi_c$, with g_d being the gauge coupling and ϕ_a ($a = 1, 2, 3$) being the adjoint scalars. As the universe expands, φ acquires a non-zero vacuum expectation value (VEV), leading to spontaneous breaking of the PQ symmetry, which is $\langle\varphi\rangle = v_\varphi$. Subsequently, the dark $SU(2)_d$ symmetry spontaneously breaks, with the triplet acquiring a non-zero VEV, $\langle\phi_3\rangle = v_\phi$. After symmetry breaking of $SU(2)_d \rightarrow U(1)_d$, there are two massive charged gauge bosons W'_\pm with $m_{W'} = g_d v_\phi$, one massless gauge boson γ' , and one massive scalar ϕ with $m_\phi = -2\lambda_{\varphi\phi}v_\varphi^2 + 3\lambda_\phi v_\phi^2$. In addition, the hidden 't Hooft-Polyakov monopole [65] may be formed.

This study explores the breaking of dark $SU(2)_d$ symmetry at different phase transition temperature scales (the sub-EeV and sub-GeV levels), which are determined by the VEV of PQ symmetry v_φ and the coupling $\lambda_{\varphi\phi}$. For simplicity in the discussion, we fixed the parameter v_φ to 10^{10} GeV in this study. The nature of the dark sector requires its coupling with the visible sector to be extremely weak. In this paper, we set the coupling constant between ϕ_3 and the axion $\lambda_{\varphi\phi} \ll 1$. To study the phase transition of dark $SU(2)_d$ symmetry, we use the standard approach by employing the thermal one-loop effective potential [136]

$$V_{\text{eff}}(\phi_3, T) = V_{\text{tree}}(\phi_3) + V_{\text{CW}}(\phi_3) + V_{\text{c.t}}(\phi_3) + V_1^{\text{T}}(\phi_3, T) + V_1^{\text{daisy}}(\phi_3, T). \quad (2.2)$$

The $V_{\text{eff}}(\phi_3, T)$ and $V_{\text{CW}}(\phi_3)$ are the tree-level potential and the 1-loop Coleman-Weinberg potential, with $V_{\text{c.t}}(\phi_3)$ to keep the zero temperature vacuum un-shifting. The finite temperature correction is described by the term $V_1^{\text{T}}(\phi_3, T)$ and the daisy correction term $V_1^{\text{daisy}}(\phi_3, T)$. The specific form of each thermal correction can be found in the Appendix A.

The characteristic temperatures of the phase transition distinguish the different stages of this process, which is crucial to understand the dynamics of the transition. The critical temperature T_c is the temperature at which the system exhibits two degenerate vacuum states in co-existence. Bubble nucleation occurs at T_n , where, on average, one bubble is nucleated within one unit horizon volume. At percolation temperature T_p , the probability of finding a point remaining in the false vacuum is 70%. At this time, it can be roughly considered as the completion of the phase transition.

The three characteristic temperatures can be determined accordingly using the definitions of these characteristics outlined above. The bubble nucleation rate Γ is defined by [123] $\Gamma \sim T^4 e^{-S_3/T} (S_3/2\pi T)^4$. And the definition of the action of the bubble solution

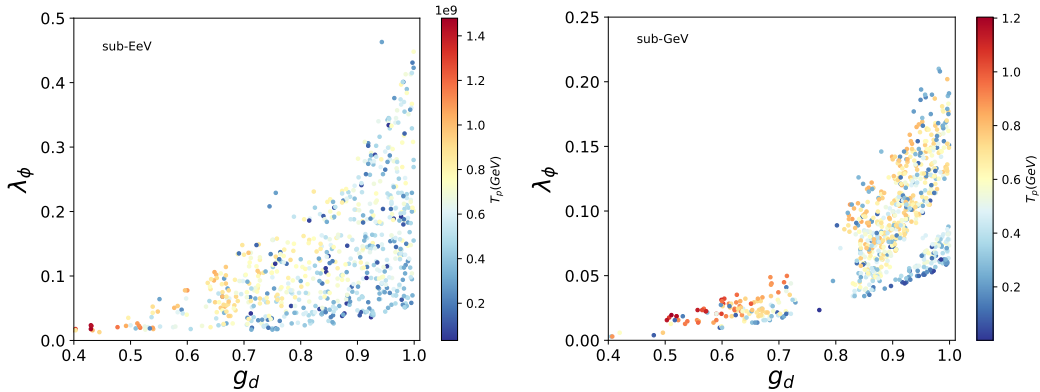


Figure 1. The left and right panels illustrate the distribution of viable parameter points in the $\lambda_\phi - g_d$ plane corresponding to phase transitions occurring at the sub-EeV and sub-GeV energy scales, respectively. The colormap on the right side of the figure represents the percolation temperature T_p of the phase transition.

S_3 is given by

$$S_3 = 4\pi \int_0^\infty dr r^2 \left[\frac{1}{2} \left(\frac{d\phi}{dr} \right)^2 + V_{\text{eff}}(\phi, T) \right], \quad (2.3)$$

where $\phi(r) = \phi_3$ is the “bounce solution” acquired from the equations of motion

$$\frac{d^2\phi}{dr^2} + \frac{2}{r} \frac{d\phi}{dr} = \frac{\partial V_{\text{eff}}}{\partial \phi}, \quad (2.4)$$

with the boundary conditions

$$\left. \frac{d\phi}{dr} \right|_{r=0} = \phi_{\text{phase 1}}, \quad \left. \frac{d\phi}{dr} \right|_{r=\infty} = \phi_{\text{phase 2}}, \quad (2.5)$$

between the two phases $\phi_{\text{phase 1}}$ (true vacuum) and $\phi_{\text{phase 2}}$ (false vacuum) during the transition. In this work, we use the FindBounce [86] package to calculate the “bounce solution”. The probability of a point remaining in the false vacuum is defined as [124, 126, 127]:

$$P(T) = \exp \left[\frac{4\pi v_w^3}{3} \int_T^{T_c} \frac{dT' \Gamma(T')}{H(T') T'^4} \left(\int_T^{T'} \frac{d\tilde{T}}{H(\tilde{T})} \right)^3 \right], \quad (2.6)$$

where v_w is the velocity of the bubble wall.

By simultaneously varying v_φ and $\lambda_{\varphi\phi}$ while keeping the product $\lambda_{\varphi\phi}(T^2 + 3v_\varphi^2)$ constant, the feasible parameters of the phase transition can be matched to scenarios with different axion decay constant f_a . Through numerical calculations, we present the viable parameter points for the first-order phase transition in Fig. 1, where the points in the left (right) figure represent the phase transition occurring around the temperature $T_p \sim \mathcal{O}(10^8)$ GeV ($T_p \sim \mathcal{O}(10^{-1})$ GeV). As shown in Fig. 1, the viable parameter space for the sub-EeV

first-order phase transition is primarily concentrated in regions with large gauge couplings $g_d > 0.4$ and small scalar self-couplings $\lambda_\phi < 0.45$. In addition, it is observed that the percolation temperature T_p tends to decrease as g_d increases. In contrast, for the sub-GeV phase transition, the viable parameter space favors smaller scalar self-couplings $\lambda_\phi < 0.2$.

3 The Witten effect and the DM relic density

During the phase transition, monopoles can form at a rate of approximately $p \sim \mathcal{O}(10^{-1})$ as vacuum bubbles collide with each other. Thus, a quantitative relationship can be established to express the number density of monopole n_M in terms of the number density of colliding bubbles n_b , which also demonstrates the crucial role of bubble collisions in the monopole production process [88],

$$n_M = pn_b = p \frac{\beta^3}{8\pi v_w^3}. \quad (3.1)$$

Hidden monopoles are formed when the $SU(2)_d$ symmetry spontaneously breaks down to $U(1)_d$. Then, the configurations of the scalar and gauge fields are presented as follows [2]:

$$\phi_a = v_\phi H(r) \frac{x_a}{r}, \quad A_i^a = \frac{1}{g_d} \frac{\epsilon^{aij} x^j}{r^2} F(r), \quad (i, j = 1, 2, 3), \quad (3.2)$$

where ϵ^{aij} is the totally antisymmetric tensor of rank 3 with a convention $\epsilon^{123} = 1$, and $r = \sqrt{x^2 + y^2 + z^2}$. In terms of the above configurations and dimensionless variable $\xi = v_\phi r$, the Lagrangian given in Eq. (2.1) reduces to

$$L = \frac{4\pi v_\phi}{g_d^2} \int_0^\infty d\xi \left[\left(\frac{dF}{d\xi} \right)^2 + \frac{2F^2(1-F)^2}{\xi^2} + \frac{F^4}{2\xi^2} + \frac{g_d^2 \xi^2}{2} \left(\frac{dH}{d\xi} \right)^2 + g_d^2 H^2 (1-F)^2 + \frac{g_d^2 V_{eff}(H)}{v_\phi^4} \xi^2 \right]. \quad (3.3)$$

The boundary conditions for the aforementioned equations of motion can be written as follows:

$$\frac{d^2 F}{d\xi^2} = \frac{F}{\xi^2} (1-F)(2-F) + g_d^2 H^2 (F-1), \quad (3.4)$$

$$\frac{d^2 H}{d\xi^2} + \frac{2}{\xi} \frac{dH}{d\xi} = \frac{2H}{\xi^2} (1-F)^2 + \frac{1}{v_\phi^4} \frac{dV_{eff}(H)}{dH}. \quad (3.5)$$

Here, the functions $H(\xi)$ and $F(\xi)$ satisfy boundary conditions:

$$\lim_{\xi \rightarrow 0} H(\xi) \rightarrow 0, \quad \lim_{\xi \rightarrow 0} F(\xi) \rightarrow 0, \quad \lim_{\xi \rightarrow \infty} H(\xi) \rightarrow 1, \quad \lim_{\xi \rightarrow \infty} F(\xi) \rightarrow 1. \quad (3.6)$$

In Fig. 2, we use BM1 from the sub-GeV scale and BM4 from the sub-EeV scale to illustrate the profiles of $H(\xi)$ and $F(\xi)$ at the percolation temperature T_p . The horizontal axis in this figure is chosen as $g_d \times \xi = r \times m_w$ to represent the core size of a monopole.

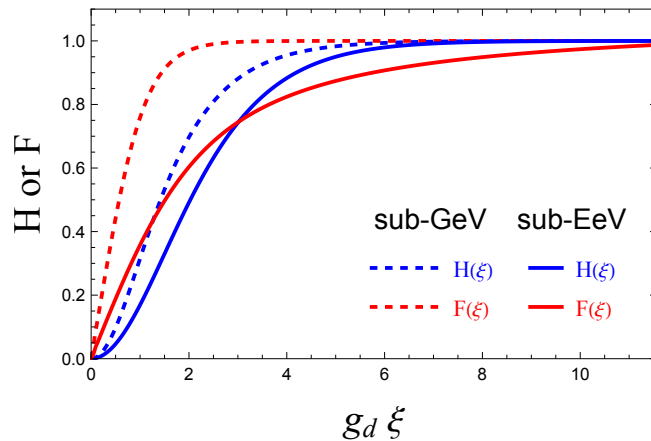


Figure 2. The blue and red curves represent the profiles of $H(\xi)$ and $F(\xi)$, respectively, where the horizontal axis corresponds to $g_d \xi = r m_w'$. The solid, and dashed lines correspond to BM1 and BM4 in the Table. 1 respectively.

With $H(\xi)$ and $F(\xi)$ being calculated numerically, the monopole mass can be calculated using the following equation,

$$m_M = \frac{4\pi v_\phi}{g_d^2} \int_0^\infty d\xi \left[\left(\frac{dF}{d\xi} \right)^2 + \frac{2F^2(1-F)^2}{\xi^2} + \frac{F^4}{2\xi^2} + \frac{g_d^2 \xi^2}{2} \left(\frac{dH}{d\xi} \right)^2 + g_d^2 H^2 (1-F)^2 + \frac{g_d^2 V_T(H)}{v_\phi^4} \xi^2 - \frac{g_d^2 V_T(H=1)}{v_\phi^4} \xi^2 \right]. \quad (3.7)$$

The attractive interaction between monopoles and antimonopoles leads to annihilation, a process known as “diffusive capture” [79, 87, 100, 101], which further impacts the monopole number density n_M . This process can take place only if the mean free path of the monopole, $\bar{\lambda}_{mfp} \sim \sqrt{m_M/T}/(BT)$, is shorter than its capture radius, $r_{cap} \sim h^2/T$ [65, 66], where B represents the drag force exerted on the monopole by the thermal plasma [79, 87, 101], and $h = 1/g_d$ denotes the hidden magnetic charge of the monopole. The situation we study is the same as that in [98], where $\bar{\lambda}_{mfp} > r_{cap}$, meaning that the annihilation of monopoles with anti-monopoles does not affect their number density n_M generated during the phase transition. Once the monopole number density n_M and mass m_M are determined, its relic density can be calculated using the definition of the density parameter, as expressed below:

$$\Omega_M h^2 = \frac{\rho_{M,0}}{\rho_{crit,0}} h^2 = p m_M \frac{\beta^3 g_s(T_0) T_0^3 h^2}{24\pi v_w^3 g_s(T_*) T_*^3 M_{pl}^2 H_0^2}, \quad (3.8)$$

where, $s_*(s_0)$ represents the entropy density of the universe at the end of phase transition(today), g_s is the effective number of degrees of freedom in entropy, and H_0 denotes the present-day Hubble constant.

As discussed above, the mass and relic density of the monopole are closely related to the energy scale of the phase transition. In the sub-GeV case, the monopole mass

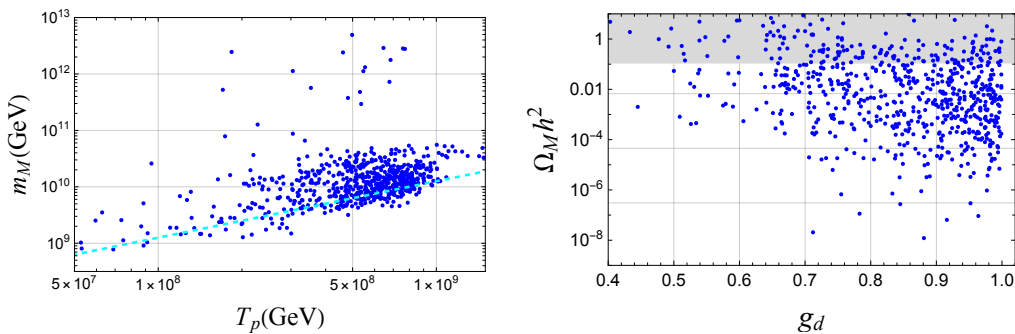


Figure 3. The left panel shows the relationship between the monopole mass m_M and the percolation temperature T_p . The cyan dashed line represents the value $4\pi T_p$, providing a reference scale for comparison. The right panel illustrates the evolution of the monopole relic density, $\Omega_M h^2$, as a function of g_d . The gray-shaded region represents the constrain of observed DM abundance [34]

and relic density are extremely minimal, rendering them unobservable. Therefore, in the subsequent discussion, we focus solely on the scenario in which the phase transition occurs at the sub-EeV scale. The left panel of Fig. 3 presents the relation between percolation temperature T_p and monopole mass m_M calculated using the formulas mentioned above. From this figure, it can be observed that the monopole mass is approximately proportional to the percolation temperature T_p , following the relation $m_M \sim 4\pi v_\phi / g_d^2 \sim 4\pi T_p$ since most points are concentrated around $v_\phi(T_p) \sim T_p$ with $g_d^2 \sim 1$. Furthermore, the right panel of Fig. 3 shows that most viable points from the sub-EeV phase transition contribute non-negligibly to the DM relic density, whereas some of the heavier monopoles are excluded by the current observed relic density [34].

In our investigation of the influence of the Witten effect on axion mass, we utilize the coupling framework consistent with that presented in [1], which describes the interaction between the axion and the dark $U(1)_d$ gauge field.

$$\mathcal{L}_\theta = -\frac{e'^2}{32\pi^2} \frac{a}{f_a} F'^{\mu\nu} \tilde{F}'_{\mu\nu}, \quad (3.9)$$

where $e' \equiv 4\pi/g_d$ is the dark electric gauge coupling. This coupling is inherited following the interaction between the axion and the dark $SU(2)_d$ gauge field. Moreover, hidden magnetic monopoles acquire hidden electric charge from this Lagrangian, transforming into particles that simultaneously possess both electric and magnetic charges, known as dyons, and this effect is called the Witten effect [105]. Furthermore, considering axions in an electromagnetic field that contains both monopoles and antimonopoles, the axion acquire an effective mass $m_{a,M}$, which is determined by the number density of monopoles [1, 103]

$$m_{a,M}^2 \simeq 2\beta \frac{n_M(T)}{f_a}, \quad (3.10)$$

where $\beta \equiv e'^2/128\pi^3 r_c f_a$, n_M is the number density of the monopole and antimonopole, $n_M = n_M^+ + n_M^-$ and r_c , the core size of the hidden monopole, can be estimated as the

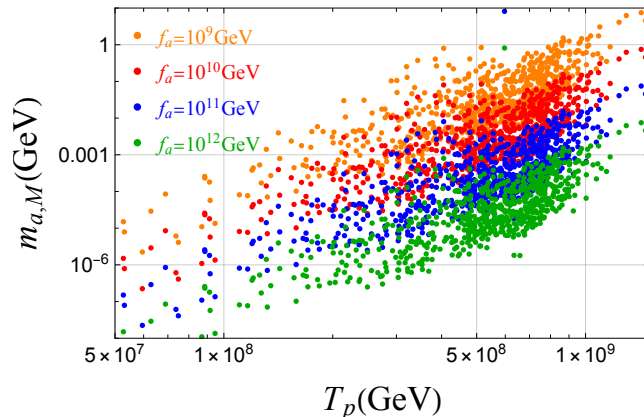


Figure 4. This figure illustrates the relationship between the percolation temperature T_p and the axion mass $m_{a,M}$ obtained via the Witten effect. The orange, red, blue, and green points represent cases where the axion decay constant $f_a = 10^9$ GeV, $f_a = 10^{10}$ GeV, $f_a = 10^{11}$ GeV, and $f_a = 10^{12}$ GeV, respectively.

inverse of the mass of the charged gauge bosons generated after the spontaneous symmetry breaking of the $SU(2)_d$ gauge symmetry. In Fig. 4, we present the relationship between the axion mass $m_{a,M}$ induced by the Witten effect and the percolation temperature T_p . As shown in Eq.(3.10), the axion mass $m_{a,M}$ is inversely proportional to the axion decay constant f_a , with most $m_{a,M}$ clustering around 10^{-3} GeV. In the sub-EeV scenario, the contribution of the Witten effect to the axion mass significantly exceeds that of the QCD effect $m_{a,QCD} \sim 5.70\mu\text{eV} \times 10^{16}\text{GeV}/f_a$ [7, 10].

In the post-inflation scenario, the breaking of global PQ symmetry may lead to the formation of topological defect, such as global strings, which release energy through radiating free axions [76, 92]. After acquiring mass through the Witten effect, the axion can be considered as cold DM. Furthermore, we refer to the study in ref. [68] to explore the contribution of KSVZ axion [78, 90] (for $N_{DW} = 1$) produced by cosmic string radiation to the axion relic density, which can be written as:

$$\Omega_{a,CS} h^2 \approx 1.6 \times 10^9 f_a^2 m_a^2 \xi \left(-2.25 + \log \frac{f_a}{m_a \xi^{1/2}} \right) \times \epsilon^{-1} \left(m_a^2 M_{\text{pl}}^2 g_*^{1/3} \right)^{-3/4}, \quad (3.11)$$

where, ξ and ϵ are dimensionless parameters determined by the simulation. Based on [68], their values are approximately $\xi \sim 0.37$ and $\epsilon \sim 0.85$.

In addition, analogously to the effects of the QCD phase transition, the Witten effect contributes to the axion mass and induces the formation of axionic domain walls [30]. Axion strings, arising from the breaking of the U(1) PQ symmetry, are attached to axionic domain walls. This configuration is known as a string-wall system, and its decay also contributes to the axion number density [77, 93]. The contribution to the DM relic abundance from DFSZ axion [90, 91] emitted by domain walls, when the domain wall number $N_{DW} > 1$,

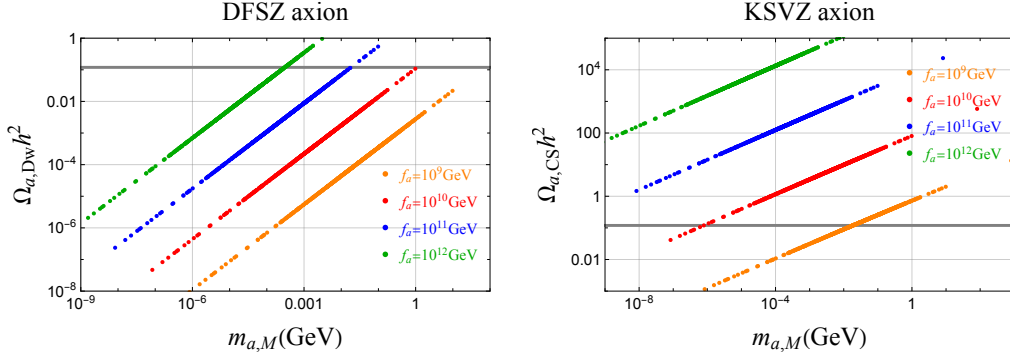


Figure 5. The left (right) panel illustrates the relationship between the abundance of DFSZ axions (KSVZ axions) and the axion mass. The orange, red, blue, and green points represent cases where the axion decay constant $f_a = 10^9$ GeV, $f_a = 10^{10}$ GeV, $f_a = 10^{11}$ GeV and $f_a = 10^{12}$ GeV, respectively.

can be described as follows [74]

$$\Omega_{a,DW}h^2 = 1.02 \times 10^{-19} \left(\frac{8}{3}\right)^{\frac{3}{2p}} \left(\frac{2p-1}{3-2p}\right) C_d^{\frac{3}{2p}-1} \left(\frac{m}{\text{GeV}}\right)^{\frac{3}{p}-\frac{3}{2}} \times \left(\frac{f_a}{\text{GeV}}\right)^{4-\frac{3}{p}} \Delta V^{1-\frac{3}{2p}} \left(\frac{\csc(\pi/N_{DW})}{N_{DW}^2}\right)^{\frac{3}{p}-2}, \quad (3.12)$$

In calculating the axion relic density, we adopted a method similar to that in ref. [74], with parameters $C_d \sim 100$, $p \sim 5/4$, and $N_{DW} = 3$.

In Fig. 5, the dependence of the abundances of the DFSZ and KSVZ axion on the mass $m_{a,M}$ and the decay constant f_a of the axion is presented. It demonstrates a positive correlation between the axion abundance $\Omega_a h^2$ and axion mass $m_{a,M}$ and the decay constant f_a . The results are shown on the right side of Fig. 5, where it is evident that the axion relic density $\Omega_{a,DW}h^2$ decreases as the axion mass $m_{a,M}$ increases. If only the DFSZ axion abundance $\Omega_{a,DW}h^2$ from domain wall decay is considered, the DFSZ axion would need to acquire a larger mass to account for the observed DM relic density. Furthermore, the contribution of domain wall decay to the DFSZ axion abundance is much smaller than that of cosmic string decay to the KSVZ axion abundance. Current experimental observations of the DM relic density exclude specific parameter ranges of KSVZ axion with larger f_a and heavier $m_{a,M}$.

4 The gravitational wave and the dark radiation

The existence of dark phase transitions and domain wall collapse processes suggests that gravitational waves emitted by these events could provide valuable insights into probing new physics models. Our primary focus is on the stochastic gravitational wave background, particularly when its peak frequency lies within the nanohertz range detectable by PTA experiments. Accordingly, we investigate domain wall gravitational waves in the sub-EeV scenario and phase transition gravitational waves in the sub-GeV scenario. Additionally,

we examine the constraints imposed by CMB observations on relativistic particles in the dark sector, commonly referred to as dark radiation.

4.1 Gravitational waves from the dark phase transition

Evaluating the gravitational wave spectrum produced during a first-order phase transition requires determining the phase transition strength parameter α and the duration parameter β , defined as follows:

$$\alpha = \frac{\rho_{\text{vac}}}{\rho_{\text{DR}}}, \quad \beta = HT \frac{dS_3/T}{dT}, \quad (4.1)$$

where $\rho_{\text{DR}} = \pi^2 g_{\text{DR}} T^4/30$ is the plasma energy density, and [122] the vacuum energy released during the phase transition is defined as below

$$\rho_{\text{vac}} = V_{\text{eff}}(\phi_{\text{phase 1}}) - V_{\text{eff}}(\phi_{\text{phase 2}}) - \frac{T}{4} \frac{\partial}{\partial T} [V_{\text{eff}}(\phi_{\text{phase 1}}) - V_{\text{eff}}(\phi_{\text{phase 2}})]. \quad (4.2)$$

Moreover, in subsequent discussions of this work, we perform the calculations at $T_* = T_p$ while adopting the notation T_* for consistency in description.

In this paper, we follow the method outlined in [54] to estimate the gravitational waves generated during the dark first-order phase transition, taking into account contributions from bubble collisions [3], sound waves [14, 18], and turbulence [17, 112].

$$\Omega_{\text{GW}} h^2 = (\Omega_{\text{bubble}} + \Omega_{\text{sw}} + \Omega_{\text{turb}}) h^2. \quad (4.3)$$

where

$$\Omega_i h^2 = \sum_i \Omega_{\text{rad},0} h^2 \left(\frac{g(T_*)}{g_0} \right) \left(\frac{g_{s0}}{g_s(T_*)} \right)^{4/3} \left(\frac{H_*}{\beta} \right)^2 \left(\frac{\kappa_i \alpha'}{1 + \alpha'} \right)^2 \tilde{\Omega}_i. \quad (4.4)$$

Here $\Omega_{\text{rad},0} h^2 = 4.16 \times 10^{-5}$ [111] with h is the reduced Hubble parameter, and α' can be defined as

$$\alpha' \equiv \frac{\rho_{\text{vac}}}{\rho_{\text{rad,tot}}(T_*)} = \frac{\rho_{\text{vac}}}{\rho_{\text{rad}}(T_*) + \rho_{\text{DR}}(T_*)} \simeq \frac{\rho_{\text{vac}}}{3H_*^2 M_p^2}, \quad (4.5)$$

where $\rho_{\text{rad,tot}}(T_*)$ is the total radiation energy density just before the phase transition.

$$\tilde{\Omega}_{\text{bubble}}(f) \simeq 1.0 \left(\frac{0.11 v_w^3}{0.42 + v_w^2} \right) \left(\frac{3.8 (f/f_{\text{bubble}})^{2.8}}{1 + 2.8 (f/f_{\text{bubble}})^{3.8}} \right), \quad (4.6)$$

$$\tilde{\Omega}_{\text{sw}}(f) \simeq 0.16 v_w \left(\frac{\beta}{H_*} \right) \Upsilon(\bar{U}_f, R_*) \left(\frac{f}{f_{\text{sw}}} \right)^3 \left(\frac{7}{4 + 3 (f/f_{\text{sw}})^2} \right)^{7/2}, \quad (4.7)$$

$$\tilde{\Omega}_{\text{turb}}(f) \simeq 20 v_w \left(\frac{\beta}{H_*} \right) \left(\frac{\kappa_{\text{turb}} \alpha'}{1 + \alpha'} \right)^{-1/2} \frac{(f/f_{\text{turb}})^3}{(1 + (f/f_{\text{turb}}))^{11/3} (1 + 8\pi f/h_*)}, \quad (4.8)$$

where, f is the frequency today, $\Upsilon = (1 - 1/\sqrt{1 + 2t_{\text{sw}} H_*})$ represents the suppression factor, τ_{sw} represents the duration of sound wave during the phase transition, as discussed

in ref. [116] $\tau_{sw} = \min [1/H_*, R_*/\bar{U}_f]$, $H_*R_* = v_w(8\pi)^{1/3}/(\beta/H_*)$, and the root-mean-square fluid velocity \bar{U}_f can be approximated as [16, 120, 121] $\bar{U}_f^2 \approx 3\kappa_\nu\alpha'/4(1+\alpha')$ and h_* is the Hubble parameter at T_* :

$$h_* \simeq 1.1 \times 10^{-8} \text{ Hz} \times \left(\frac{T_*}{0.1 \text{ GeV}} \right) \left(\frac{g(T_*)}{10.75} \right)^{1/2} \left(\frac{g_s(T_*)}{10.75} \right)^{-1/3}. \quad (4.9)$$

The peak frequencies of three sources f_{bubble} , f_{sw} , and f_{turb} can be written as:

$$f_{\text{bubble}} \simeq 1.1 \times 10^{-8} \text{ Hz} \left(\frac{0.62}{1.8 - 0.1v_w + v_w^2} \right) \left(\frac{\beta}{H_*} \right) \left(\frac{T_*}{0.1 \text{ GeV}} \right) \left(\frac{g(T_*)}{10.75} \right)^{1/2} \left(\frac{g_s(T_*)}{10.75} \right)^{-1/3}, \quad (4.10)$$

$$f_{\text{sw}} \simeq 1.3 \times 10^{-8} \text{ Hz} \times \frac{1}{v_w} \left(\frac{\beta}{H_*} \right) \left(\frac{T_*}{0.1 \text{ GeV}} \right) \left(\frac{g(T_*)}{10.75} \right)^{1/2} \left(\frac{g_s(T_*)}{10.75} \right)^{-1/3}, \quad (4.11)$$

$$f_{\text{turb}} \simeq 1.9 \times 10^{-8} \text{ Hz} \times \frac{1}{v_w} \left(\frac{\beta}{H_*} \right) \left(\frac{T_*}{0.1 \text{ GeV}} \right) \left(\frac{g(T_*)}{10.75} \right)^{1/2} \left(\frac{g_s(T_*)}{10.75} \right)^{-1/3}, \quad (4.12)$$

4.2 Gravitational waves from the domain wall

To prevent the universe from over-closing, a biased potential ΔV can be introduced to ensure that domain walls collapse after their formation. Furthermore, the gravitational wave signals generated during the collapse of these domain walls offer a novel avenue to test this process experimentally. This mechanism provides a new theoretical framework and experimental direction for investigating the properties of cosmological defects and their potential observational signatures. The energy released during this process is radiated as gravitational waves, and the peak frequency and peak amplitude of these waves at the present time t_0 can be estimated as follows: [128, 129]:

$$f^{dw}(t_0)_{\text{peak}} = \frac{a(t_{\text{dec}})}{a(t_0)} H(t_{\text{dec}}) \simeq 3.99 \times 10^{-9} \text{ Hz} \mathcal{A}^{-1/2} \left(\frac{1 \text{ TeV}^3}{\sigma_{\text{wall}}} \right)^{1/2} \left(\frac{\Delta V}{1 \text{ MeV}^4} \right)^{1/2} \quad (4.13)$$

$$\Omega_{\text{GW}}^{dw} h^2(t_0)_{\text{peak}} \simeq 5.20 \times 10^{-20} \times \tilde{\epsilon}_{\text{gw}} \mathcal{A}^4 \left(\frac{10.75}{g_*} \right)^{1/3} \left(\frac{\sigma_{\text{wall}}}{1 \text{ TeV}^3} \right)^4 \left(\frac{1 \text{ MeV}^4}{\Delta V} \right)^2 \quad (4.14)$$

where $\sigma_{\text{wall}} \sim c_a m_{a,M} f_a^2$, $c_a = \mathcal{O}(1)$ is a numerical constant. The bias term ΔV introduced in Eqs. (4.13) and (4.14) explicitly breaks the discrete symmetry, which determines the decay time of the domain wall.

$$t_{\text{dec}} \approx \mathcal{A} \sigma_{\text{wall}} / (\Delta V). \quad (4.15)$$

Furthermore, another constraint is that domain wall collapse must occur before Big Bang Nucleosynthesis (BBN), that is, $t_{\text{dec}} \leq 0.01 \text{ sec}$ [113, 114]. This condition places a lower limit on the bias term:

$$\Delta V \gtrsim 6.6 \times 10^{-2} \text{ MeV}^4 \mathcal{A} \left(\frac{\sigma_{\text{wall}}}{1 \text{ TeV}^3} \right). \quad (4.16)$$

Naturally, the bias term has not only a lower bound but also an upper bound. Specifically, the magnitude of the bias term must be much smaller than the potential around the core

of the domain walls ($\Delta V \ll V$), ensuring that the discrete symmetry is approximately preserved. In this paper, based on the case of $N_{\text{dw}} = 3$, we selected the area parameter $\mathcal{A} = 1.2$ [128] and the efficiency parameter $\tilde{\epsilon}_{\text{gw}} = 0.7$ [129], which are consistent with the \mathbb{Z}_3 discrete symmetry. According to the literature [129], after calculating the peak frequency and peak amplitude of the gravitational waves, the domain wall gravitational wave power spectrum can be approximated as a piecewise function: for $f < f_{\text{peak}}^{\text{dw}}$, $\Omega_{\text{GW}}^{\text{dw}} h^2 \propto f^3$, and for $f \geq f_{\text{peak}}^{\text{dw}}$, $\Omega_{\text{GW}}^{\text{dw}} h^2 \propto f^{-1}$.

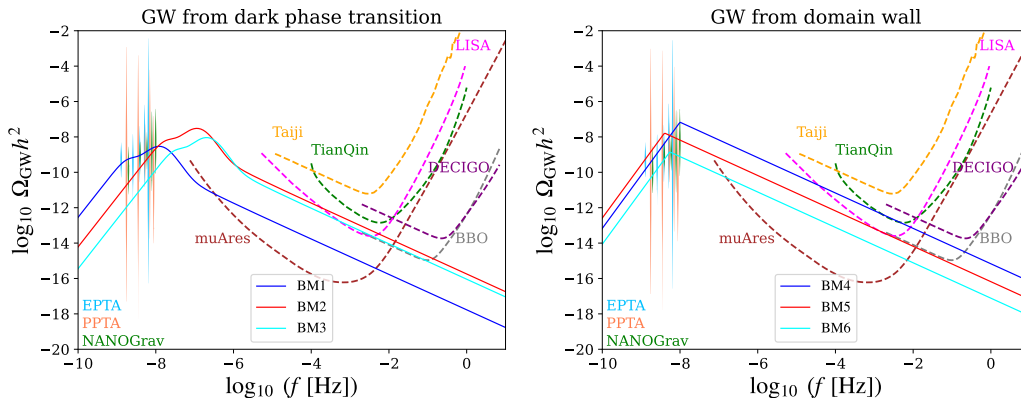


Figure 6. The left panel illustrates the gravitational wave energy spectra generated by dark phase transitions for the first three benchmark points listed in Table 1. Meanwhile, the right panel depicts the gravitational wave energy spectra resulting from axion domain wall decay for the last three benchmark points in Table 1. The violin plots represent data from three experiments: EPTA [138], PPTA [139], and NANOGrav [137]. Moreover the brown, gray, orange, green, purple and gray dashed lines show the projected sensitivity of the muAres [67], LISA [72, 73], Taiji [69, 71], TianQin [70], DECIGO [104, 106, 107] and BBO [102] collaboration, respectively.

We present the predictions for phase-transition gravitational waves and domain wall collapse gravitational waves at several benchmark points from Table 1 in Fig. 6. As shown in this figure, the peak frequencies of both types of gravitational waves lie within the nanohertz range, making them detectable by current PTA experiments and future space-based gravitational wave detectors. Table 1 presents six viable parameter points for the

	gd	λ_ϕ	$\lambda_{\varphi\phi}$	T_p (GeV)	β/H_p	$\alpha[T_p]$
BM_1	0.771	0.023	3.91×10^{-26}	0.001	76.47	35.57
BM_2	0.972	0.054	1.05×10^{-22}	0.038	23.36	114.67
BM_3	0.927	0.046	4.49×10^{-23}	0.038	41.24	25.84
BM_4	0.903	0.064	5.407×10^{-4}	4.798×10^8	563.75	0.012
BM_5	0.916	0.097	2.512×10^{-6}	3.847×10^7	2030.55	0.0039
BM_6	0.833	0.049	1.875×10^{-5}	9.455×10^7	617.42	0.013

Table 1. Benchmarks in the Fig. 6.

first-order phase transition. The first three correspond to phase transition at the sub-GeV

scale, while the last three are associated with sub-EeV scale phase transition.

4.3 Dark radiation

This study assumes that the dark sector does not directly couple to the visible sector but is connected through the axion as a mediator particle. In the sub-GeV scenario, the coupling between the dark sector and the axion is extremely weak, implying that the interactions between the dark and visible sectors are negligible. In the sub-EeV scenario, the dark and visible sectors decouple from thermal equilibrium after the axion decouples from the SM. Since the coupling strength between the axion and the SM is significantly suppressed by f_a , it can be inferred that the decoupling between the dark sector and the visible sector occurs before the electroweak phase transition. Furthermore, after the first-order phase transition, it is reasonable to assume that the entropy of the dark and visible sectors are separately conserved, which allows us to write the following relation:

$$\frac{g_s^d(T_d)T_d^3}{g_s^d(T_{D,d})T_{D,d}^3} = \frac{g_s^{sm}(T_{sm})T_{sm}^3}{g_s^{sm}(T_{D,sm})T_{D,sm}^3}. \quad (4.17)$$

where $g^{sm}(T)(g_s^{sm}(T))$ and $g^d(T)(g_s^d(T))$ are the relativistic degrees of freedom for the energy (entropy) densities in the visible and dark sectors. When we assume that the first-order phase transition does not occur under supercooling conditions, the extra effective number of relativistic particles can be reasonably expressed as follows [54]:

$$\Delta N_{eff} \simeq 0.49 \times \left(\frac{R}{0.13}\right)^{4/3} \left(\frac{g_0^d}{g_0^{sm}}\right) \left(\frac{g_{s,0}^{sm}}{g_{s,0}^d}\right)^{4/3}, \quad (4.18)$$

where $R = s_d(T)/s_{sm}(T)|_{T>T_{pt}}$, the subscript 0 represents the value at the recombination epoch.

After the breaking of dark symmetry, the dark photon remains massless, whereas the axion mass depending on the specific scenario. For the sub-EeV dark phase transition, the Witten effect gives the axion a substantial mass, rendering it incompatible with the criteria for dark radiation and leading to $\Delta N_{eff} = 0.46$. However, in the case of a sub-GeV phase transition, the axion acquires a much smaller mass from both non-perturbative QCD effect and the Witten effect, which remains far below the temperature $m_a < T_*$. In this scenario, both the dark photon and the axion can be considered as dark radiation, yielding $\Delta N_{eff} = 0.40$. Current observations from Planck and BBO provide the constraint [34, 89] $N_{eff} = 3.27 \pm 0.15$. In the SM, $N_{eff} = 3.046$. Moreover, refs. [34, 75, 96] suggest that $\Delta N_{eff} \sim 0.4 - 0.5$ could effectively alleviate tension in the Hubble constant.

5 Conclusion and Discussions

In this study, we explore the generation of hidden monopoles through spontaneous breaking of dark $SU(2)_d$ symmetry, focusing on their effects on axion mass and the viability of monopoles and axions as candidates for DM. We also examine the potential of current

gravitational wave experiments to detect stochastic gravitational wave backgrounds arising from dark $SU(2)_d$ phase transitions and axionic domain wall collapse.

Our study indicates that in the sub-EeV scenario, the mass of hidden monopoles is around 10^{10} GeV, making them viable DM candidates. Furthermore, the axion mass induced by the Witten effect ranges from 10^{-5} GeV to 10^{-1} GeV, with its precise value determined by the axion decay constant f_a . The Witten effect contributes significantly more to the axion mass than the non-perturbative QCD effects, making the axion a compelling cold DM candidate. In this scenario, axions radiated by domain walls, their relic density is below the current observation across most of the viable phase-transition parameter space. When the axion decay constant f_a is sufficiently large, such as 10^{11} or 10^{12} GeV, the DFSZ axion can satisfy the correct relic density. On the other hand, for axions radiated by cosmic strings, their relic density in most of the viable phase-transition parameter space is excluded by the observed relic density. Only when the axion decay constant f_a is sufficiently small, such as 10^9 or 10^{10} GeV, can the KSVZ axion align with current experimental results. In the sub-GeV scenario, the monopole-induced contribution to the axion mass becomes negligible compared to the contribution from non-perturbative QCD effects. In this case, the axion mass is primarily determined by the QCD instanton effect.

In addition, it is worth noting that in the sub-GeV scenario, the stochastic gravitational wave background from the cosmological first-order phase transition and in the sub-EeV scenario, the stochastic gravitational wave background from axionic domain wall collapse both have peak frequencies in the nano-Hertz range, offering a potential explanation for the low-frequency gravitational wave signals observed by the EPTA, PPTA, and NANOGrav collaborations. This also opens up a new avenue for exploring new physics models that include this dark sector.

Additionally, if the axionic domain wall interacts with lepton or baryon currents, their formation and collapse could facilitate the generation of lepton or baryon number asymmetry, offering a potential explanation for the observed baryon asymmetry in the universe. This mechanism referred to as “DW-genesis” in refs [94, 95], represents a novel production mechanism. Meanwhile, the contribution of the Witten effect to the axion mass may impact the axiogenesis [8, 9] process, where the cosmological net baryon number is generated via the rotation of the QCD axion. We leave this topic to future work.

A Thermal correction

The Coleman-Weinberg contribution can be written as [135]

$$V_{\text{CW}}(\phi) = \sum_i \frac{g_i (-1)^b}{64\pi^2} m_i^4(\phi) \left(\text{Log} \left[\frac{m_i^2(\phi)}{\Lambda_{UV}^2} \right] - C_i \right), \quad (\text{A.1})$$

where $b = 0(1)$ for bosons (fermions), Λ_{UV} is the \overline{MS} renormalization scale, $g_i = \{1, 1, 6\}$ for the $\{\phi, G_{W'}, W'\}$ in this model, $C_i = 5/6$ for gauge boson, and $C_i = 3/2$ for others.

$$V_{\text{c.t}} = \delta\mu\phi^2 + \delta\lambda\phi^4, \quad (\text{A.2})$$

where the corresponding coefficients calculated by

$$\frac{\partial V_{\text{c.t.}}}{\partial \phi} + \frac{\partial V_{\text{CW}}}{\partial \phi} \Big|_{\phi \rightarrow v_\phi} = 0, \quad \frac{\partial^2 V_{\text{c.t.}}}{\partial \phi^2} + \frac{\partial^2 V_{\text{CW}}}{\partial \phi^2} \Big|_{\phi \rightarrow v_\phi} = 0. \quad (\text{A.3})$$

The one-loop finite temperature corrections can be written as [134]

$$V_1^T(\phi, T) = \frac{T^4}{2\pi^2} \sum_i n_i J_B \left(\frac{m_i^2(\phi)}{T^2} \right), \quad (\text{A.4})$$

where the functions J_B are

$$J_B(y) = \int_0^\infty dx x^2 \ln \left[1 - \exp \left(-\sqrt{x^2 + y} \right) \right], \quad (\text{A.5})$$

with $y \equiv m_i^2(\phi)/T^2$.

The thermal integrals J_B defined in Eq. (A.5) can be expressed as an infinite series involving modified Bessel functions of the second kind $K_n(x)$ with $n = 2$ [133],

$$J_B(y) = \lim_{N \rightarrow +\infty} - \sum_{l=1}^N \frac{y}{l^2} K_2(\sqrt{yl}). \quad (\text{A.6})$$

The daisy term $V_1^{\text{daisy}}(\phi, T)$ is given by [130, 131]

$$V_1^{\text{daisy}}(\phi, T) = -\frac{T}{12\pi} \sum_{i=\text{bosons}} n_i \left[(m_i^2(\phi) + c_i(T))^{\frac{3}{2}} - (m_i^2(\phi))^{\frac{3}{2}} \right], \quad (\text{A.7})$$

where the finite temperature corrections are given by

$$c_\phi(T) = \frac{1}{12} T^2 (6g_d^2 + 5\lambda_\phi), \quad c_{W'}(T) = \frac{11}{6} g_d^2 T^2. \quad (\text{A.8})$$

Acknowledgments

This work is supported by the National Key Research and Development Program of China under Grant No. 2021YFC2203004. R.Z. is supported by the National Natural Science Foundation of China under Grant No. 12305109, by Science and Technology Research Project of Chongqing Municipal Education Commission under Grant No. KJQN202300614, and by the National Natural Science Foundation of China under Grant No. 12147102. L.B. is supported by the National Natural Science Foundation of China under Grants Nos. 12322505, 12347101, L.B. also acknowledges Chongqing Natural Science Foundation under Grant No. CSTB2024NSCQ-JQX0022 and Chongqing Talents: Exceptional Young Talents Project No. cstc2024ycjhbzxm0020.

References

- [1] W. Fischler and J. Preskill, *DYON - AXION DYNAMICS*, *Phys. Lett. B* **125** (1983) 165.
- [2] T. Hiramatsu, M. Ibe, M. Suzuki and S. Yamaguchi, *Gauge kinetic mixing and dark topological defects*, *JHEP* **12** (2021) 122 [2109.12771].

- [3] S.J. Huber and T. Konstandin, *Gravitational Wave Production by Collisions: More Bubbles*, *JCAP* **09** (2008) 022 [[0806.1828](#)].
- [4] C. Caprini et al., *Science with the space-based interferometer eLISA. II: Gravitational waves from cosmological phase transitions*, *JCAP* **04** (2016) 001 [[1512.06239](#)].
- [5] P.J. Steinhardt, *Relativistic Detonation Waves and Bubble Growth in False Vacuum Decay*, *Phys. Rev. D* **25** (1982) 2074.
- [6] M. Kamionkowski, A. Kosowsky and M.S. Turner, *Gravitational radiation from first order phase transitions*, *Phys. Rev. D* **49** (1994) 2837 [[astro-ph/9310044](#)].
- [7] G. Grilli di Cortona, E. Hardy, J. Pardo Vega and G. Villadoro, *The QCD axion, precisely*, *JHEP* **01** (2016) 034 [[1511.02867](#)].
- [8] R.T. Co and K. Harigaya, *Axiogenesis*, *Phys. Rev. Lett.* **124** (2020) 111602 [[1910.02080](#)].
- [9] R.T. Co, T. Gherghetta and K. Harigaya, *Axiogenesis with a heavy QCD axion*, *JHEP* **10** (2022) 121 [[2206.00678](#)].
- [10] A. Hook, *TASI Lectures on the Strong CP Problem and Axions*, *PoS TASI2018* (2019) 004 [[1812.02669](#)].
- [11] PIERRE AUGER collaboration, *Search for ultrarelativistic magnetic monopoles with the Pierre Auger Observatory*, *Phys. Rev. D* **94** (2016) 082002 [[1609.04451](#)].
- [12] N.E. Mavromatos and V.A. Mitsou, *Magnetic monopoles revisited: Models and searches at colliders and in the Cosmos*, *Int. J. Mod. Phys. A* **35** (2020) 2030012 [[2005.05100](#)].
- [13] ICECUBE collaboration, *Searches for Relativistic Magnetic Monopoles in IceCube*, *Eur. Phys. J. C* **76** (2016) 133 [[1511.01350](#)].
- [14] M. Hindmarsh, S.J. Huber, K. Rummukainen and D.J. Weir, *Numerical simulations of acoustically generated gravitational waves at a first order phase transition*, *Phys. Rev. D* **92** (2015) 123009 [[1504.03291](#)].
- [15] M. Hindmarsh, S.J. Huber, K. Rummukainen and D.J. Weir, *Gravitational waves from the sound of a first order phase transition*, *Phys. Rev. Lett.* **112** (2014) 041301 [[1304.2433](#)].
- [16] J. Ellis, M. Lewicki, J.M. No and V. Vaskonen, *Gravitational wave energy budget in strongly supercooled phase transitions*, *JCAP* **06** (2019) 024 [[1903.09642](#)].
- [17] C. Caprini, R. Durrer and G. Servant, *The stochastic gravitational wave background from turbulence and magnetic fields generated by a first-order phase transition*, *JCAP* **12** (2009) 024 [[0909.0622](#)].
- [18] M.B. Hindmarsh, M. Lüben, J. Lumma and M. Pauly, *Phase transitions in the early universe*, *SciPost Phys. Lect. Notes* **24** (2021) 1 [[2008.09136](#)].
- [19] S. Nakagawa, F. Takahashi and M. Yamada, *Cosmic Birefringence Triggered by Dark Matter Domination*, *Phys. Rev. Lett.* **127** (2021) 181103 [[2103.08153](#)].
- [20] M.L. Graesser, I.M. Shoemaker and N.T. Arellano, *Milli-magnetic monopole dark matter and the survival of galactic magnetic fields*, *JHEP* **03** (2022) 105 [[2105.05769](#)].
- [21] Y. Nomura, S. Rajendran and F. Sanches, *Axion Isocurvature and Magnetic Monopoles*, *Phys. Rev. Lett.* **116** (2016) 141803 [[1511.06347](#)].
- [22] R. Caldwell et al., *Detection of early-universe gravitational-wave signatures and fundamental physics*, *Gen. Rel. Grav.* **54** (2022) 156 [[2203.07972](#)].

- [23] D. Borah, A. Dasgupta and S.K. Kang, *A first order dark $SU(2)_D$ phase transition with vector dark matter in the light of NANOGrav 12.5 yr data*, *JCAP* **12** (2021) 039 [[2109.11558](#)].
- [24] V.V. Khoze and G. Ro, *Dark matter monopoles, vectors and photons*, *JHEP* **10** (2014) 061 [[1406.2291](#)].
- [25] Y. Bai, M. Korwar and N. Orlofsky, *Electroweak-Symmetric Dark Monopoles from Preheating*, *JHEP* **07** (2020) 167 [[2005.00503](#)].
- [26] S. Baek, P. Ko and W.-I. Park, *Hidden sector monopole, vector dark matter and dark radiation with Higgs portal*, *JCAP* **10** (2014) 067 [[1311.1035](#)].
- [27] J. Terning and C.B. Verhaaren, *Detecting Dark Matter with Aharonov-Bohm*, *JHEP* **12** (2019) 152 [[1906.00014](#)].
- [28] J. Evslin and S.B. Gudnason, *Dwarf Galaxy Sized Monopoles as Dark Matter?*, [1202.0560](#).
- [29] H. Murayama and J. Shu, *Topological Dark Matter*, *Phys. Lett. B* **686** (2010) 162 [[0905.1720](#)].
- [30] M. Kawasaki, F. Takahashi and M. Yamada, *Suppressing the QCD Axion Abundance by Hidden Monopoles*, *Phys. Lett. B* **753** (2016) 677 [[1511.05030](#)].
- [31] C. Gomez Sanchez and B. Holdom, *Monopoles, strings and dark matter*, *Phys. Rev. D* **83** (2011) 123524 [[1103.1632](#)].
- [32] L. Delle Rose, G. Panico, M. Redi and A. Tesi, *Gravitational Waves from Supercool Axions*, *JHEP* **04** (2020) 025 [[1912.06139](#)].
- [33] M. Punturo et al., *The Einstein Telescope: A third-generation gravitational wave observatory*, *Class. Quant. Grav.* **27** (2010) 194002.
- [34] PLANCK collaboration, *Planck 2018 results. VI. Cosmological parameters*, *Astron. Astrophys.* **641** (2020) A6 [[1807.06209](#)].
- [35] LIGO SCIENTIFIC, VIRGO collaboration, *Search for the isotropic stochastic background using data from Advanced LIGO's second observing run*, *Phys. Rev. D* **100** (2019) 061101 [[1903.02886](#)].
- [36] C.S. Machado, W. Ratzinger, P. Schwaller and B.A. Stefanek, *Gravitational wave probes of axionlike particles*, *Phys. Rev. D* **102** (2020) 075033 [[1912.01007](#)].
- [37] P.S.B. Dev and A. Mazumdar, *Probing the Scale of New Physics by Advanced LIGO/VIRGO*, *Phys. Rev. D* **93** (2016) 104001 [[1602.04203](#)].
- [38] B. Von Harling, A. Pomarol, O. Pujolàs and F. Rompineve, *Peccei-Quinn Phase Transition at LIGO*, *JHEP* **04** (2020) 195 [[1912.07587](#)].
- [39] R. Sato, F. Takahashi and M. Yamada, *Unified Origin of Axion and Monopole Dark Matter, and Solution to the Domain-wall Problem*, *Phys. Rev. D* **98** (2018) 043535 [[1805.10533](#)].
- [40] R. Daido, S.-Y. Ho and F. Takahashi, *Hidden monopole dark matter via axion portal and its implications for direct detection searches, beam-dump experiments, and the H_0 tension*, *JHEP* **01** (2020) 185 [[1909.03627](#)].
- [41] I. Baldes and C. Garcia-Cely, *Strong gravitational radiation from a simple dark matter model*, *JHEP* **05** (2019) 190 [[1809.01198](#)].

- [42] EPTA, INPTA: collaboration, *The second data release from the European Pulsar Timing Array - III. Search for gravitational wave signals*, *Astron. Astrophys.* **678** (2023) A50 [2306.16214].
- [43] D.J. Reardon et al., *Search for an Isotropic Gravitational-wave Background with the Parkes Pulsar Timing Array*, *Astrophys. J. Lett.* **951** (2023) L6 [2306.16215].
- [44] Y. Bai, S. Lu and N. Orlofsky, *Searching for Magnetic Monopoles with the Earth's Magnetic Field*, *Phys. Rev. Lett.* **127** (2021) 101801 [2103.06286].
- [45] C. Zhang, S.-H. Zhang, B. Fu, J.-F. Zhang and X. Zhang, *On the cosmological abundance of magnetic monopoles*, *JHEP* **08** (2024) 220 [2404.04926].
- [46] A. Addazi, Y.-F. Cai, A. Marciano and L. Visinelli, *Have pulsar timing array methods detected a cosmological phase transition?*, *Phys. Rev. D* **109** (2024) 015028 [2306.17205].
- [47] P. Athron, A. Fowlie, C.-T. Lu, L. Morris, L. Wu, Y. Wu et al., *Can Supercooled Phase Transitions Explain the Gravitational Wave Background Observed by Pulsar Timing Arrays?*, *Phys. Rev. Lett.* **132** (2024) 221001 [2306.17239].
- [48] Y.-M. Wu, Z.-C. Chen and Q.-G. Huang, *Cosmological interpretation for the stochastic signal in pulsar timing arrays*, *Sci. China Phys. Mech. Astron.* **67** (2024) 240412 [2307.03141].
- [49] S. He, L. Li, S. Wang and S.-J. Wang, *Constraints on holographic QCD phase transitions from PTA observations*, *Sci. China Phys. Mech. Astron.* **68** (2025) 210411 [2308.07257].
- [50] Z.-C. Chen, S.-L. Li, P. Wu and H. Yu, *NANOGrav hints for first-order confinement-deconfinement phase transition in different QCD-matter scenarios*, *Phys. Rev. D* **109** (2024) 043022 [2312.01824].
- [51] X. Xue et al., *Constraining Cosmological Phase Transitions with the Parkes Pulsar Timing Array*, *Phys. Rev. Lett.* **127** (2021) 251303 [2110.03096].
- [52] W. Ratzinger and P. Schwaller, *Whispers from the dark side: Confronting light new physics with NANOGrav data*, *SciPost Phys.* **10** (2021) 047 [2009.11875].
- [53] A. Addazi, Y.-F. Cai, Q. Gan, A. Marciano and K. Zeng, *NANOGrav results and dark first order phase transitions*, *Sci. China Phys. Mech. Astron.* **64** (2021) 290411 [2009.10327].
- [54] Y. Nakai, M. Suzuki, F. Takahashi and M. Yamada, *Gravitational Waves and Dark Radiation from Dark Phase Transition: Connecting NANOGrav Pulsar Timing Data and Hubble Tension*, *Phys. Lett. B* **816** (2021) 136238 [2009.09754].
- [55] L. Bian, R.-G. Cai, J. Liu, X.-Y. Yang and R. Zhou, *Evidence for different gravitational-wave sources in the NANOGrav dataset*, *Phys. Rev. D* **103** (2021) L081301 [2009.13893].
- [56] H. Xu et al., *Searching for the Nano-Hertz Stochastic Gravitational Wave Background with the Chinese Pulsar Timing Array Data Release I*, *Res. Astron. Astrophys.* **23** (2023) 075024 [2306.16216].
- [57] NANOGrav collaboration, *The NANOGrav 15 yr Data Set: Evidence for a Gravitational-wave Background*, *Astrophys. J. Lett.* **951** (2023) L8 [2306.16213].
- [58] C.-H. Chen and T. Nomura, *Searching for vector dark matter via Higgs portal at the LHC*, *Phys. Rev. D* **93** (2016) 074019 [1507.00886].

- [59] E. Hall, T. Konstandin, R. McGehee, H. Murayama and G. Servant, *Baryogenesis From a Dark First-Order Phase Transition*, *JHEP* **04** (2020) 042 [[1910.08068](#)].
- [60] C.-W. Chiang, T. Nomura and J. Tandean, *Nonabelian Dark Matter with Resonant Annihilation*, *JHEP* **01** (2014) 183 [[1306.0882](#)].
- [61] M.L. Graesser and J.K. Osiński, *Hidden Sector Monopole Dark Matter with Matter Domination*, *JHEP* **11** (2020) 133 [[2007.07917](#)].
- [62] C.-H. Chen and T. Nomura, *$SU(2)_X$ vector DM and Galactic Center gamma-ray excess*, *Phys. Lett. B* **746** (2015) 351 [[1501.07413](#)].
- [63] P. Ko, T. Nomura and H. Okada, *Dark matter physics in dark $SU(2)$ gauge symmetry with non-Abelian kinetic mixing*, *Phys. Rev. D* **103** (2021) 095011 [[2007.08153](#)].
- [64] J. Fan, K. Fraser, M. Reece and J. Stout, *Axion Mass from Magnetic Monopole Loops*, *Phys. Rev. Lett.* **127** (2021) 131602 [[2105.09950](#)].
- [65] G. 't Hooft, *Magnetic Monopoles in Unified Gauge Theories*, *Nucl. Phys. B* **79** (1974) 276.
- [66] A.M. Polyakov, *Particle Spectrum in Quantum Field Theory*, *JETP Lett.* **20** (1974) 194.
- [67] A. Sesana et al., *Unveiling the gravitational universe at μ -Hz frequencies*, *Exper. Astron.* **51** (2021) 1333 [[1908.11391](#)].
- [68] Y. Jia and L. Bian, *Gravitational wave and dark matter from Axion-Higgs string*, [2412.04218](#).
- [69] W.-H. Ruan, Z.-K. Guo, R.-G. Cai and Y.-Z. Zhang, *Taiji program: Gravitational-wave sources*, *Int. J. Mod. Phys. A* **35** (2020) 2050075 [[1807.09495](#)].
- [70] TIANQIN collaboration, *TianQin: a space-borne gravitational wave detector*, *Class. Quant. Grav.* **33** (2016) 035010 [[1512.02076](#)].
- [71] W.-R. Hu and Y.-L. Wu, *The Taiji Program in Space for gravitational wave physics and the nature of gravity*, *Natl. Sci. Rev.* **4** (2017) 685.
- [72] J. Baker et al., *The Laser Interferometer Space Antenna: Unveiling the Millihertz Gravitational Wave Sky*, [1907.06482](#).
- [73] LISA collaboration, *Laser Interferometer Space Antenna*, [1702.00786](#).
- [74] Y. Li, L. Bian, R.-G. Cai and J. Shu, *Cosmic Simulations of Axion String-Wall Networks: Probing Dark Matter and Gravitational Waves for Discovery*, [2311.02011](#).
- [75] J.L. Bernal, L. Verde and A.G. Riess, *The trouble with H_0* , *JCAP* **10** (2016) 019 [[1607.05617](#)].
- [76] T. Hiramatsu, M. Kawasaki, T. Sekiguchi, M. Yamaguchi and J. Yokoyama, *Improved estimation of radiated axions from cosmological axionic strings*, *Phys. Rev. D* **83** (2011) 123531 [[1012.5502](#)].
- [77] M. Kawasaki, K. Saikawa and T. Sekiguchi, *Axion dark matter from topological defects*, *Phys. Rev. D* **91** (2015) 065014 [[1412.0789](#)].
- [78] J.E. Kim, *Weak Interaction Singlet and Strong CP Invariance*, *Phys. Rev. Lett.* **43** (1979) 103.
- [79] J.T. Goldman, E.W. Kolb and D. Toussaint, *Gravitational Clumping and the Annihilation of Monopoles*, *Phys. Rev. D* **23** (1981) 867.

- [80] C. Gross, O. Lebedev and Y. Mambrini, *Non-Abelian gauge fields as dark matter*, *JHEP* **08** (2015) 158 [[1505.07480](#)].
- [81] C. Boehm, M.J. Dolan and C. McCabe, *A weighty interpretation of the Galactic Centre excess*, *Phys. Rev. D* **90** (2014) 023531 [[1404.4977](#)].
- [82] T. Hambye, *Hidden vector dark matter*, *JHEP* **01** (2009) 028 [[0811.0172](#)].
- [83] A. Vilenkin, *Gravitational Field of Vacuum Domain Walls and Strings*, *Phys. Rev. D* **23** (1981) 852.
- [84] S.E. Larsson, S. Sarkar and P.L. White, *Evading the cosmological domain wall problem*, *Phys. Rev. D* **55** (1997) 5129 [[hep-ph/9608319](#)].
- [85] G.B. Gelmini, M. Gleiser and E.W. Kolb, *Cosmology of Biased Discrete Symmetry Breaking*, *Phys. Rev. D* **39** (1989) 1558.
- [86] V. Guada, M. Nemevšek and M. Pintar, *FindBounce: Package for multi-field bounce actions*, *Comput. Phys. Commun.* **256** (2020) 107480 [[2002.00881](#)].
- [87] J. Preskill, *Cosmological Production of Superheavy Magnetic Monopoles*, *Phys. Rev. Lett.* **43** (1979) 1365.
- [88] M.B. Einhorn and K. Sato, *Monopole Production in the Very Early Universe in a First Order Phase Transition*, *Nucl. Phys. B* **180** (1981) 385.
- [89] A.G. Riess, S. Casertano, W. Yuan, L. Macri, J. Anderson, J.W. MacKenty et al., *New parallaxes of galactic cepheids from spatially scanning the hubble space telescope: Implications for the hubble constant*, *The Astrophysical Journal* **855** (2018) 136.
- [90] M.A. Shifman, A.I. Vainshtein and V.I. Zakharov, *Can Confinement Ensure Natural CP Invariance of Strong Interactions?*, *Nucl. Phys. B* **166** (1980) 493.
- [91] A.R. Zhitnitsky, *On Possible Suppression of the Axion Hadron Interactions. (In Russian)*, *Sov. J. Nucl. Phys.* **31** (1980) 260.
- [92] M. Yamaguchi, M. Kawasaki and J. Yokoyama, *Evolution of axionic strings and spectrum of axions radiated from them*, *Phys. Rev. Lett.* **82** (1999) 4578 [[hep-ph/9811311](#)].
- [93] D.H. Lyth, *Estimates of the cosmological axion density*, *Phys. Lett. B* **275** (1992) 279.
- [94] M. Vanvlasselaer, *DW-genesis: generating the baryon number from domain walls*, 12, 2024 [[2501.00491](#)].
- [95] A. Mariotti, X. Nagels, A. Rase and M. Vanvlasselaer, *DW-genesis: baryon number from domain wall network collapse*, [2411.13494](#).
- [96] N. Blinov and G. Marques-Tavares, *Interacting radiation after Planck and its implications for the Hubble Tension*, *JCAP* **09** (2020) 029 [[2003.08387](#)].
- [97] B. Julia and A. Zee, *Poles with Both Magnetic and Electric Charges in Nonabelian Gauge Theory*, *Phys. Rev. D* **11** (1975) 2227.
- [98] A. Banerjee and M.A. Buen-Abad, *Dynamical Axion Misalignment from the Witten Effect*, [2410.21369](#).
- [99] K.S. Jeong, S. Nakagawa, F. Takahashi and M. Yamada, *Dissipation of axion energy via the Schwinger and Witten effects*, *Phys. Rev. D* **109** (2024) 015014 [[2309.16570](#)].
- [100] Y.B. Zeldovich and M.Y. Khlopov, *On the Concentration of Relic Magnetic Monopoles in the Universe*, *Phys. Lett. B* **79** (1978) 239.

- [101] A. Vilenkin and E.P.S. Shellard, *Cosmic Strings and Other Topological Defects*, Cambridge University Press (7, 2000).
- [102] J. Crowder and N.J. Cornish, *Beyond LISA: Exploring future gravitational wave missions*, *Phys. Rev. D* **72** (2005) 083005 [[gr-qc/0506015](#)].
- [103] M. Kawasaki, F. Takahashi and M. Yamada, *Adiabatic suppression of the axion abundance and isocurvature due to coupling to hidden monopoles*, *JHEP* **01** (2018) 053 [[1708.06047](#)].
- [104] N. Seto, S. Kawamura and T. Nakamura, *Possibility of direct measurement of the acceleration of the universe using 0.1-Hz band laser interferometer gravitational wave antenna in space*, *Phys. Rev. Lett.* **87** (2001) 221103 [[astro-ph/0108011](#)].
- [105] E. Witten, *Dyons of Charge $e\theta/2\pi$* , *Phys. Lett. B* **86** (1979) 283.
- [106] S. Kawamura et al., *Current status of space gravitational wave antenna DECIGO and B-DECIGO*, *PTEP* **2021** (2021) 05A105 [[2006.13545](#)].
- [107] H. Kudoh, A. Taruya, T. Hiramatsu and Y. Himemoto, *Detecting a gravitational-wave background with next-generation space interferometers*, *Phys. Rev. D* **73** (2006) 064006 [[gr-qc/0511145](#)].
- [108] B. Fornal, Y. Shirman, T.M.P. Tait and J.R. West, *Asymmetric dark matter and baryogenesis from $SU(2)_\ell$* , *Phys. Rev. D* **96** (2017) 035001 [[1703.00199](#)].
- [109] L. Bian, H.-K. Guo, Y. Wu and R. Zhou, *Gravitational wave and collider searches for electroweak symmetry breaking patterns*, *Phys. Rev. D* **101** (2020) 035011 [[1906.11664](#)].
- [110] T. Ghosh, H.-K. Guo, T. Han and H. Liu, *Electroweak phase transition with an $SU(2)$ dark sector*, *JHEP* **07** (2021) 045 [[2012.09758](#)].
- [111] D.J. Fixsen, *The Temperature of the Cosmic Microwave Background*, *Astrophys. J.* **707** (2009) 916 [[0911.1955](#)].
- [112] P. Binetruy, A. Bohe, C. Caprini and J.-F. Dufaux, *Cosmological Backgrounds of Gravitational Waves and eLISA/NGO: Phase Transitions, Cosmic Strings and Other Sources*, *JCAP* **06** (2012) 027 [[1201.0983](#)].
- [113] M. Kawasaki, K. Kohri and T. Moroi, *Big-Bang nucleosynthesis and hadronic decay of long-lived massive particles*, *Phys. Rev. D* **71** (2005) 083502 [[astro-ph/0408426](#)].
- [114] M. Kawasaki, K. Kohri and T. Moroi, *Hadronic decay of late - decaying particles and Big-Bang Nucleosynthesis*, *Phys. Lett. B* **625** (2005) 7 [[astro-ph/0402490](#)].
- [115] Y. Di, J. Wang, R. Zhou, L. Bian, R.-G. Cai and J. Liu, *Magnetic Field and Gravitational Waves from the First-Order Phase Transition*, *Phys. Rev. Lett.* **126** (2021) 251102 [[2012.15625](#)].
- [116] J. Ellis, M. Lewicki and J.M. No, *Gravitational waves from first-order cosmological phase transitions: lifetime of the sound wave source*, *JCAP* **07** (2020) 050 [[2003.07360](#)].
- [117] J.R. Espinosa, T. Konstandin, J.M. No and G. Servant, *Energy Budget of Cosmological First-order Phase Transitions*, *JCAP* **06** (2010) 028 [[1004.4187](#)].
- [118] D. Cutting, M. Hindmarsh and D.J. Weir, *Gravitational waves from vacuum first-order phase transitions: from the envelope to the lattice*, *Phys. Rev. D* **97** (2018) 123513 [[1802.05712](#)].

- [119] D. Cutting, E.G. Escartin, M. Hindmarsh and D.J. Weir, *Gravitational waves from vacuum first order phase transitions II: from thin to thick walls*, *Phys. Rev. D* **103** (2021) 023531 [[2005.13537](#)].
- [120] C. Caprini et al., *Detecting gravitational waves from cosmological phase transitions with LISA: an update*, *JCAP* **03** (2020) 024 [[1910.13125](#)].
- [121] M. Hindmarsh, S.J. Huber, K. Rummukainen and D.J. Weir, *Shape of the acoustic gravitational wave power spectrum from a first order phase transition*, *Phys. Rev. D* **96** (2017) 103520 [[1704.05871](#)].
- [122] K. Enqvist, J. Ignatius, K. Kajantie and K. Rummukainen, *Nucleation and bubble growth in a first order cosmological electroweak phase transition*, *Phys. Rev. D* **45** (1992) 3415.
- [123] X. Wang, F.P. Huang and X. Zhang, *Phase transition dynamics and gravitational wave spectra of strong first-order phase transition in supercooled universe*, *JCAP* **05** (2020) 045 [[2003.08892](#)].
- [124] A.H. Guth and E.J. Weinberg, *Cosmological Consequences of a First Order Phase Transition in the $SU(5)$ Grand Unified Model*, *Phys. Rev. D* **23** (1981) 876.
- [125] J.M. Moreno, M. Quiros and M. Seco, *Bubbles in the supersymmetric standard model*, *Nucl. Phys. B* **526** (1998) 489 [[hep-ph/9801272](#)].
- [126] A.H. Guth and S.H.H. Tye, *Phase Transitions and Magnetic Monopole Production in the Very Early Universe*, *Phys. Rev. Lett.* **44** (1980) 631.
- [127] L. Leitaó, A. Megevand and A.D. Sanchez, *Gravitational waves from the electroweak phase transition*, *JCAP* **10** (2012) 024 [[1205.3070](#)].
- [128] K. Kadota, M. Kawasaki and K. Saikawa, *Gravitational waves from domain walls in the next-to-minimal supersymmetric standard model*, *JCAP* **10** (2015) 041 [[1503.06998](#)].
- [129] T. Hiramatsu, M. Kawasaki and K. Saikawa, *On the estimation of gravitational wave spectrum from cosmic domain walls*, *JCAP* **02** (2014) 031 [[1309.5001](#)].
- [130] P.B. Arnold and O. Espinosa, *The Effective potential and first order phase transitions: Beyond leading-order*, *Phys. Rev. D* **47** (1993) 3546 [[hep-ph/9212235](#)].
- [131] M.E. Carrington, *The Effective potential at finite temperature in the Standard Model*, *Phys. Rev. D* **45** (1992) 2933.
- [132] R. Hlozek, D. Grin, D.J.E. Marsh and P.G. Ferreira, *A search for ultralight axions using precision cosmological data*, *Phys. Rev. D* **91** (2015) 103512 [[1410.2896](#)].
- [133] G.W. Anderson and L.J. Hall, *The Electroweak phase transition and baryogenesis*, *Phys. Rev. D* **45** (1992) 2685.
- [134] L. Dolan and R. Jackiw, *Symmetry Behavior at Finite Temperature*, *Phys. Rev. D* **9** (1974) 3320.
- [135] S.R. Coleman and E.J. Weinberg, *Radiative Corrections as the Origin of Spontaneous Symmetry Breaking*, *Phys. Rev. D* **7** (1973) 1888.
- [136] M. Quiros, *Finite temperature field theory and phase transitions*, in *ICTP Summer School in High-Energy Physics and Cosmology*, pp. 187–259, 1, 1999 [[hep-ph/9901312](#)].
- [137] NANOGrav collaboration, *The NANOGrav 12.5 yr Data Set: Search for an Isotropic Stochastic Gravitational-wave Background*, *Astrophys. J. Lett.* **905** (2020) L34 [[2009.04496](#)].

- [138] EPTA collaboration, *Common-red-signal analysis with 24-yr high-precision timing of the European Pulsar Timing Array: inferences in the stochastic gravitational-wave background search*, *Mon. Not. Roy. Astron. Soc.* **508** (2021) 4970 [[2110.13184](#)].
- [139] B. Goncharov et al., *On the Evidence for a Common-spectrum Process in the Search for the Nanohertz Gravitational-wave Background with the Parkes Pulsar Timing Array*, *Astrophys. J. Lett.* **917** (2021) L19 [[2107.12112](#)].
- [140] G. 't Hooft, *Computation of the Quantum Effects Due to a Four-Dimensional Pseudoparticle*, *Phys. Rev. D* **14** (1976) 3432.
- [141] A. Vilenkin and A.E. Everett, *Cosmic Strings and Domain Walls in Models with Goldstone and PseudoGoldstone Bosons*, *Phys. Rev. Lett.* **48** (1982) 1867.
- [142] P. Sikivie, *Of Axions, Domain Walls and the Early Universe*, *Phys. Rev. Lett.* **48** (1982) 1156.
- [143] Y.B. Zeldovich, I.Y. Kobzarev and L.B. Okun, *Cosmological Consequences of the Spontaneous Breakdown of Discrete Symmetry*, *Zh. Eksp. Teor. Fiz.* **67** (1974) 3.
- [144] J. Preskill, M.B. Wise and F. Wilczek, *Cosmology of the Invisible Axion*, *Phys. Lett. B* **120** (1983) 127.
- [145] F. Wilczek, *Problem of Strong P and T Invariance in the Presence of Instantons*, *Phys. Rev. Lett.* **40** (1978) 279.
- [146] S. Weinberg, *A New Light Boson?*, *Phys. Rev. Lett.* **40** (1978) 223.
- [147] R.D. Peccei and H.R. Quinn, *Constraints Imposed by CP Conservation in the Presence of Instantons*, *Phys. Rev. D* **16** (1977) 1791.
- [148] R.D. Peccei and H.R. Quinn, *CP Conservation in the Presence of Instantons*, *Phys. Rev. Lett.* **38** (1977) 1440.
- [149] C. Vafa and E. Witten, *Parity Conservation in QCD*, *Phys. Rev. Lett.* **53** (1984) 535.